

Viscoelastic Behavior of Semicrystalline Thermoplastic Polymers during the Early Stages of Crystallization

Salvatore Coppola, Stefano Acierno, and Nino Grizzuti*

Dipartimento di Ingegneria Chimica, Università di Napoli Federico II, Piazzale Tecchio 80, I-80125 Napoli, Italy

Dimitris Vlassopoulos

FORTH, Institute of Electronic Structure & Laser and University of Crete, Department of Materials Science & Technology, Heraklion 71110, Crete, Greece

Received August 23, 2005; Revised Manuscript Received December 14, 2005

ABSTRACT: Using rheological techniques, we investigate the evolution of the microstructure evolution during the early stages of quiescent crystallization of poly(1-butene). In performing the measurements, use is made of an innovative experimental protocol, called “inverse quenching”, which allows stopping the crystallization process and producing a stable biphasic (crystalline/amorphous) system. In this way, very low frequency measurements at fixed degrees of crystallization are made possible. We find that crystallization, evidenced as a liquid-to-solid transition (LST) under isothermal conditions, with characteristics of critical gel behavior, takes place at surprisingly low degrees of crystallinity (below 1.5%). The critical gel properties, which are found to depend on both crystallization temperature and molecular weight, can be reduced to a single master curve when the gel strength is plotted as a function of the relaxation exponent. More importantly, the LST is preceded by the development of a long relaxation process. This latter process, although not fully understood, brings analogies to the slow dynamics observed in hybrid colloid–polymer systems (block copolymer micelles or multiarm star polymers) as well as the recently suggested presence of dormant nuclei. It is clear, however, that the connectivity among crystallites, apparently via the amorphous segments, plays a key role in this new process.

1. Introduction

When cooled below the thermodynamic melting temperature, thermoplastic polymers undergo crystallization. The early stages of this process are characterized by a gradual change in the material mechanical response from a liquidlike to a solidlike behavior, which is a consequence of the microstructural evolution of the system. This fact has several implications, including those related to processing applications, where information on the evolving crystallinity is crucially necessary.

In view of the above, it is not surprising that rheological techniques have been increasingly used in the past two decades as a tool for the study of polymer crystallization, often coupled to other, more traditional methods such as X-ray scattering, dilatometry and differential scanning calorimetry (DSC). One major feature of rheological measurements is their high sensitivity to microstructural changes. This allows, for example, the measurement of the early stage crystallization kinetics, where DSC may fail due to the small amount of crystallinity developed and, therefore, to the low heat flux involved.

One way to rheologically monitor crystallization is by means of dynamic mechanical spectroscopy (DMS). In this case, small-amplitude oscillatory shear (SAOS) flow is applied to the sample during its phase transition. The orders-of-magnitude increase of the storage modulus is often directly related to the degree of crystallization by assuming a direct proportionality between the relative crystallinity, α , and a reduced storage modulus:^{1–3}

$$\alpha = \frac{X}{X_{\infty}} = \frac{G' - G'_0}{G'_{\infty} - G'_0} \quad (1)$$

In eq 1, X is the crystal volume fraction, X_{∞} is its maximum value, and G'_0 and G'_{∞} are the elastic moduli at the beginning and at completion of crystallization, respectively. If quiescent crystallization kinetics are to be investigated, both deformation and frequency must be suitably chosen in order to avoid flow-induced crystallization.⁴

A more advanced use of SAOS experiments involves the determination of the so-called critical gel point. It was first recognized by Winter and co-workers that polymer crystallization can be viewed as a physical gelation process.⁵ Within this framework, the transition between liquidlike and solidlike behavior takes place at the critical gel point, where the relaxation modulus, $G(t)$, is given by

$$G(t) = St^{-n} \quad \text{for } \lambda_0 < t < +\infty \quad (2)$$

where S is the gel stiffness, n is the critical relaxation exponent, and λ_0 is the time of crossover to some faster dynamics. By means of eq 2, it is possible to predict all linear viscoelastic properties at the gel point. In particular, the loss tangent is given by

$$\tan \delta = \frac{G''}{G'} = \tan\left(\frac{n\pi}{2}\right) \quad \text{for } \omega < 1/\lambda_0 \quad (3)$$

The gel point, therefore, can be determined from the condition of frequency independence of the loss tangent, at least in the limit of low frequencies. The idea of a sol–gel transition to describe the crystallization process has been applied to several systems, including polyolefins,^{6,7} polyesters,⁸ and thermoplastic polyurethanes.⁹

Despite the large number of experimental studies, a clear understanding of the link between the evolving crystalline

* Corresponding author. E-mail: nino.grizzuti@unina.it.

Table 1. Some Relevant Physical Properties of the PB Samples

sample	M_n [g/mol]	M_w [g/mol]	M_w/M_n	tacticity (% mmmm)	T_m [°C]	η_0^a [Pa s]	τ_{max}^a [s]	$\Delta E/R$ [K]
PB398	106000	398000	3.8	82.7	138.4	41780	250	7190
PB177	54000	177000	3.3	79.5	134.0	3120	20	6800

^a At $T_{ref} = 140$ °C.

microstructure and the material mechanical response is still missing. Several authors^{1,3,10–12} suggest that the crystallizing melt can be seen as equivalent to a system of solid particles (the spherulites) suspended into a liquid matrix (the polymer melt). This appealingly simple idea, however, is somewhat in contrast with the experimental evidence that critical changes in the rheological behavior (like the sol–gel transition) take place at low crystallinity levels, where spherulites are small and definitely noninteracting.^{6,7,13,14} Horst and Winter¹⁵ suggested three different possibilities to explain the liquid-to-solid transition: (i) immediate contact between structural units (i.e., crystallite impingement), (ii) a network of bridging molecules which have segments in neighboring crystalline phases, or (iii) impingement of amorphous chains, immobilized by their segment attachment within a crystalline structure, with similarly immobilized chains from adjacent structures. More recently, Acierno et al.⁷ proposed an analogy between the crystallizing polymer and a system of multiarm polymer stars growing from a matrix of linear chains.

In this paper, the early stages of isotactic poly(1-butene) crystallization from the melt under quiescent conditions are investigated by means of DMS measurements. The main objective of this study is to gain a deeper understanding of the rheological evolution corresponding to the ongoing phase transition process. To this end, some advanced experimental techniques were used. On one hand, use was made of the *Multiwave*¹⁶ testing feature, which allows for the simultaneous measurement of the viscoelastic properties at different oscillation frequencies. In this way, a better determination of the apparent critical gel point was possible, due to the shorter measuring times. On the other hand, a recently proposed experimental protocol was employed, called “inverse quenching”, which allows for long time measurements at a constant degree of crystallization. Such a method was used to determine the viscoelastic behavior of the crystallizing melt at extremely low frequencies, which would have been not possible by traditional methods.

2. Experimental Section

2.1. Materials. Two commercial grades of isotactic poly(1-butene) (PB) of different molecular weight from Shell, here labeled as PB398 and PB177, were used as model polymers for this study. Some relevant properties of the polymers, summarized in Table 1, were kindly provided by Alfonso,¹⁷ except for the rheological properties that were measured in the course of this work. Disk-shaped samples for rheological experiments were prepared from as-received pellets by molding the polymers at 160 °C either in a vacuum or under a dry nitrogen atmosphere. No influence of sample preparation was observed. Dry nitrogen was also used for the rheological and optical measurements in order to prevent thermo-oxidative degradation of the material.

Sample PB177 was also filled with glass beads to prepare a model suspension. Mixing was done in a Haake Rheomix 600 for 10 min at 100 rpm and took place at a temperature of 160 °C. Glass beads had an average size of 60 μ m and were mixed to the polymer to a volume fraction of 12%. This resulted in a number bead density of about 1.06×10^6 beads/cm³.

2.2. Measurements. All rheological measurements were carried out on a strain-controlled rotational rheometer (ARES, TA Instru-

ments Inc.) equipped with a dual range force rebalance transducer (2KFRTN1). A parallel plate geometry was used with two diameters, 8 and 25 mm, to reach a good compromise between having a high torque signal and avoiding the instrument compliance at low temperatures and high frequencies. Sample thickness was always in the range 0.8–1 mm for the 8 mm plate and 1–1.5 mm for the 25 mm plate. Temperature was controlled by a nitrogen-fed convection oven. INVAR tools were used to minimize thermal expansion. In the experiments where a thermal history was applied to the sample, the gap was always varied to account for tool thermal expansion.

To efficiently probe the time-evolving viscoelastic behavior of the material during crystallization, the multiple wave dynamic test feature (*Multiwave*) of the ARES rheometer was used.¹⁶ The test is practically equivalent to a dynamic frequency sweep but requires a much shorter experimental time. The technique is based on the assumption that, within the linear regime, the total strain applied on the sample is the sum of several independent strain functions, each described by a sinusoidal wave with its own frequency (Boltzmann superposition principle). In the case of the *Multiwave* test, several frequencies, which are higher-order harmonics of the fundamental frequency, ω_i , are simultaneously applied. The storage and loss moduli at each discrete frequency are obtained by means of a discrete Fourier transform of the stress response to the compound strain. Using this technique, the experimental time needed for a frequency sweep is considerably shortened. It is then possible to sweep a range of about 3 decades of frequencies in a fraction of the time required for a normal dynamic frequency sweep. This method made it possible to obtain small “mutation numbers”,⁶ that is, the ratio between the time necessary for a single frequency sweep and the phase transition characteristic time, thus allowing for an accurate determination of the gel time at relatively low temperatures, which could not be otherwise accessible by the standard frequency sweep test.

For the optical observations samples of 200 μ m thickness were placed in a Linkam cell (CSS 450, Linkam Scientific Instruments Ltd.) and observed using a polarizing microscope (Axioscope 2 Plus, Carl Zeiss Inc.) equipped with 10 \times and 20 \times magnification objectives. Images were collected through a CCD camera (TMC-76S, Pulnix Inc), digitized by means of a frame grabber (PCI-1409, National Instruments Corp.), and stored on a personal computer. Quantitative analysis of the digital images was carried out using the software Image ProPlus.

3. Rheology of the Molten Polymers

Linear viscoelastic characterization was performed on the molten samples in the range of temperatures between 110 and 200 °C. The lower limit was determined by the minimum temperature (far below the equilibrium melting point T_m , see Table 1), at which crystallization was still not detected within the time necessary for the dynamic frequency sweep test, thus guaranteeing that the polymer was still in the melt state. The upper limit was determined by the polymer thermal degradation. Time–temperature superposition was used to reduce all data at the reference temperature of 140 °C, as shown in Figure 1. The horizontal shift factor, a_T , was determined for both materials and found to be well described by an Arrhenius-like expression. As expected, very similar values for the activation energies, ΔE , were found for the two polymers (see Table 1).

Figure 1 clearly shows the effect of sample molecular weight. The higher M_w sample displays a much higher viscosity and

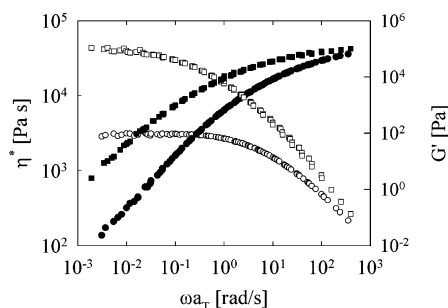


Figure 1. Complex viscosity (empty symbols) and storage modulus (filled symbols) master curves at the reference temperature of 140 °C: (○, ●) PB177; (□, ■) PB398.

reaches terminal behavior at much lower frequencies. Viscoelastic data were fitted by a multimode Maxwell model. In this way, the plateau modulus and the disentanglement time were determined. The latter was taken to be equal to the longest relaxation time, τ_{\max} , from the multimode Maxwell fitting. As the molecular weight distribution is roughly similar for the two PB's and their M_w is well above the critical molecular weight, M_c , the same values for the plateau modulus are expected, as confirmed also by visual inspection of Figure 1. Furthermore, both the longest relaxation times and of the zero-shear-rate viscosities of the two samples (reported in Table 1) scaled with the 3.2 power of the M_w ratio. Despite sample polydispersity, such a value is close to the classical 3.4 exponent that is found for monodisperse entangled polymers.¹⁹

4. Critical Gel Point and Crystallization Kinetics

The polymer crystallization kinetics under isothermal conditions were monitored by determining the gel characteristic time. To this end, the following experimental protocol was adopted. After an annealing period of 10 min at 160 °C to erase any crystalline memory, the melt was rapidly cooled (−10 °C/min) to the crystallization temperature T_c . A sequence of *Multiwave* frequency sweeps was then started at selected times $t - t_0$, where t_0 is the instant when the crystallization temperature is first reached. The gel point was determined from the condition of frequency independence of the loss tangent, at least in the low limit of the frequency window used for these experiments. Following previous studies,^{3,6,7,9} the lower bound for the frequency was set at 5×10^{-2} rad/s. The condition of constant $\tan \delta$ is equivalent to the parallelism of the $\log G'$ and $\log G''$ curves when plotted vs $\log \omega$. The relaxation exponent n and the stiffness S of the critical gel were subsequently calculated by moduli data fitting.

It should be stressed here that conditions for the critical gel point hold for frequencies smaller than $1/\lambda_0$, λ_0 being the time of crossover to some faster dynamics. In practice, λ_0 is the time over which eqs 2 and 3 should be valid. Although λ_0 is of great importance for the gel point determination, a precise physical meaning for this quantity is still lacking. We believe reasonable that λ_0 should be comparable to the experimental $G'-G''$ crossover characteristic time, as the latter is representative of overall chain relaxation. In this work, therefore, it is assumed that

$$\lambda_0 \approx \frac{1}{\omega_x} \quad (4)$$

where ω_x is the crossover frequency at the crystallization temperature.

Figure 2 demonstrates the determination of the gel point at a crystallization temperature of 98 °C for the PB177 sample. The

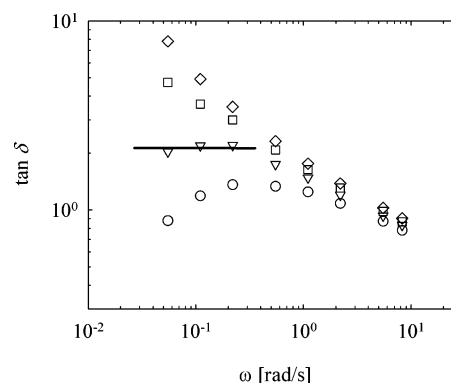


Figure 2. Loss tangent as a function of frequency during the isothermal crystallization of PB177 at 98 °C at different crystallization times, $t - t_0$: (◇) 800, (□) 13 200, (▽) 13 900, and (○) 14 600 s. In this case, the critical gel point is reached when $t - t_0 = 13\,900$ s.

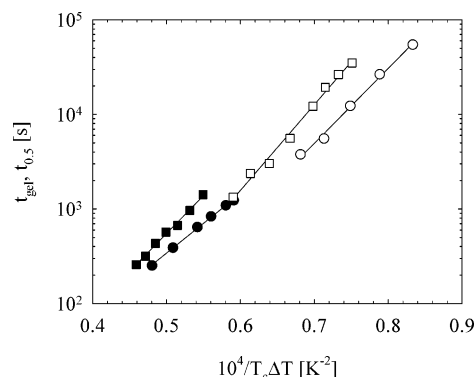


Figure 3. Rheological gel times (empty symbols) and DSC half-crystallization times (filled symbols) as a function of $1/T_c \Delta T$: (●, ○) PB177; (■, □) PB398. Solid lines through the data points are linear regression fits of the experimental results.

solid line indicates the gel point, corresponding to a frequency-independent loss tangent at low frequencies. It should be stressed here that the results shown in Figure 2 must be taken with due caution. As it will become clearer in a subsequent section, where much lower frequencies will be probed by means of the inverse quenching technique, this apparent critical gel state is not representative of the full phase transition picture.

The gel times, t_{gel} , of the two PB samples are reported in Figure 3 as a function of $1/T_c \Delta T$, where $\Delta T = T_m - T_c$ is the degree of undercooling. In the same figure the half-crystallization times, $t_{0.5}$, as obtained from DSC experiments,¹⁷ are also reported for comparison. The complementarity between DSC and rheological data is apparent. At high undercoolings the rheological t_{gel} could not be measured as it became comparable to the time needed to achieve temperature stabilization when the sample was cooled from the melt. Conversely, at lower ΔT 's, the calorimetric $t_{0.5}$ could not be determined as DSC heat fluxes were too low, thus falling below instrument sensitivity. It should be stressed that the absolute values of DSC and rheological characteristic times cannot be directly compared. As it will be discussed in a later section, critical gels are formed at very low degrees of crystallinity, much before than the 50% value of relative crystallinity (corresponding to $t_{0.5}$) has been reached.

Figure 3 shows that, in absolute terms, the lower M_w PB177 sample has faster kinetics than PB398 if the comparison is made at the same ΔT . Cortazar and Guzman²⁰ found the same trend for the half-crystallization times of poly(1-butene) samples with different molecular weights.

According to classical crystallization theories,²¹ for low degrees of undercooling a characteristic time for crystallization

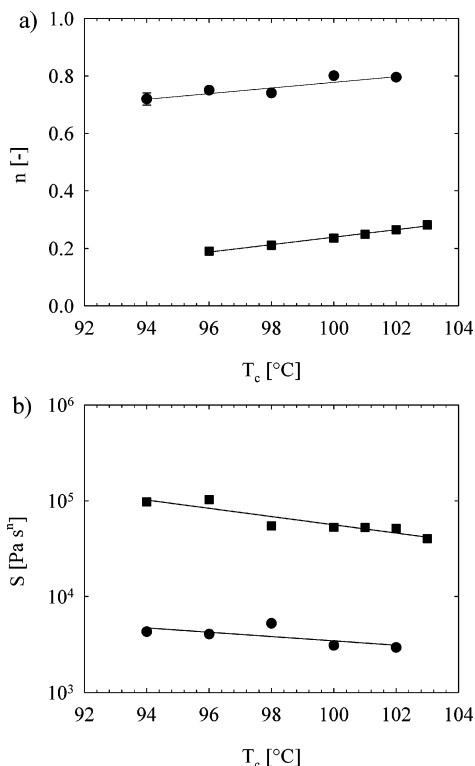


Figure 4. Relaxation exponent (a) and the strength (b) of the critical gel as a function of the crystallization temperature for the PB177 (●) and PB398 (■) samples. Solid lines are linear regression fits.

(such as $t_{0.5}$ or t_{gel}) should depend on temperature according to the following relationship:

$$t_{cryst} \propto \exp\left(\frac{K}{T_c \Delta T}\right) \quad (5)$$

where K is a crystallization rate constant. Equation 5 is indeed obeyed by the data shown in Figure 4. They also indicate that the crystallization rate of the higher MW polymer is more sensitive to temperature changes than the lower MW sample. The slopes of the t_{gel} regression lines, however, are larger than those of the $t_{0.5}$ data (about 10% for PB398 and 20% for PB177), thus indicating that rheology detects a larger temperature sensitivity of the crystallization rate. Earlier studies on PB crystallization²² indicate that the crystallization rate parameter, K , is a constant over the entire range of temperatures here investigated. Therefore, a single slope of the linear regression line should be found for each sample. The reason for the observed discrepancy remains unclear. It should be noticed, however, that similar differences between DSC and rheological characteristic time behavior was also reported by Pogodina and Winter⁶ for a series of isotactic polypropylenes.

They justified this result by speculating that $t_{0.5}$ is determined by the growth rate of the overall crystallinity, whereas t_{gel} is mainly influenced by the radial growth rate of the spherulites. The stronger temperature dependence of the gel time was attributed to crystallization being highly effective in generating long-range connectivity.

From gel point viscoelastic data the relaxation exponent and the gel stiffness were determined. Their dependence upon the crystallization temperature is reported in Figure 4. As in other previous studies,^{6,7} the scattering of these experimental derived parameters is not negligible. The trends, however, are well-defined and unambiguous. Figure 4 shows that the relaxation exponent linearly increases with temperature. Conversely, the

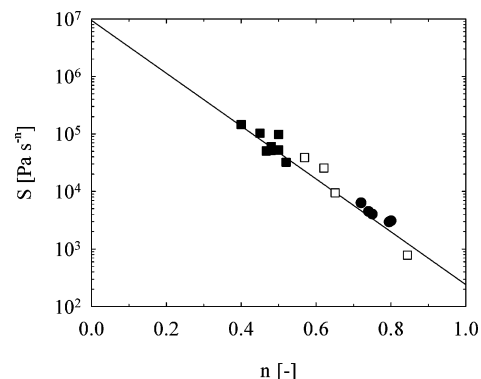


Figure 5. Gel strength as a function of the gel critical exponent at various crystallization temperatures for the PB177 (●) and PB398 (■) samples. Data by Acierio et al.⁷ (empty symbols) for PB's of different molecular weight at $T_c = 103$ °C are also reported for comparison. The solid line is a linear regression of all experimental data.

log of the gel strength is a linear decreasing function of temperature. In other words, increasing the temperature, the critical gel becomes softer and relaxes faster. Figure 4 also indicates that, at a given temperature, stronger and slower gels are obtained from the higher molecular weight sample. These results are in line with those already obtained on similar crystallizing polyolefine systems.^{6,7,15}

A more intriguing feature of the critical gel parameters can be appreciated in Figure 5, where the gel strength is plotted as a function of the relaxation exponent. All data points for the PB samples fall on the same “universal” straight line (on a log–linear scale), independently of either M_w and T_c . More strength to this feature is given by the data of Acierio et al.,⁷ who measured S and n for a series of four PB's of different M_w 's at one crystallization temperature, $T_c = 103$ °C. These data are also included in Figure 5. At the moment, we have no clear explanation for the behavior reported in Figure 5, which has been also observed for other crystallizing polymers.²³ The data seem to suggest, however, that the critical gel response is dictated by some intrinsic feature of the system, rather than by the chosen, specific physical conditions (such as the crystallization temperature or the polymer molecular weight).

5. Microstructure Development by Inverse Quenching

In this section, the microstructural evolution of the crystallizing polymer is followed in more detail by viscoelastic measurements carried out around the critical gel point. The section is structured as follows: first, the inverse quenching technique is presented, along with the determination of the optimal inverse quenching temperature. Then, the procedure to determine the relative degree of crystallinity, α , from the time evolution of the elastic modulus is discussed. Finally, viscoelastic measurements at fixed values of α are presented and discussed. Results of this section refer to sample PB177 only. In particular, crystallization was performed at the temperature of 94 °C.

5.1. Inverse Quenching. To follow the development of the crystalline microstructure through the early stages of the process, the inverse quenching technique was applied to obtain stable samples at fixed degree of crystallization. The inverse quenching is an experimental protocol that allows stopping (“quench”) the crystallization process and produce a stable biphasic (crystalline + amorphous) system. The technique is based on the observation that the crystallization rate is a function of the degree of undercooling, ΔT , and that for low values of ΔT the crystallization rate decreases as the temperature increases. Further details on this innovative methodology can be found elsewhere.¹⁴

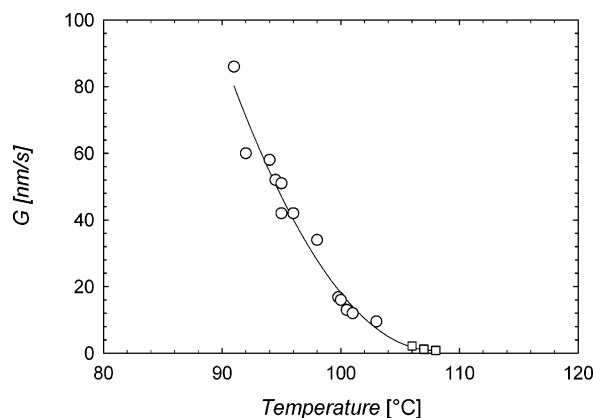


Figure 6. Spherulitic growth rate as a function of temperature for the PB177. Squared symbols represent data as obtained from the two-step procedure described in the text. The solid line through data points is only meant to guide the eye.

To achieve inverse quenching, the following thermal protocol is applied: the polymer is rapidly cooled below the melting temperature, T_m , to the crystallization temperature, T_c . After a given time, the temperature is rapidly raised to a value, T_{iq} , which is still lower than T_m . With this thermal protocol, crystallization first proceeds at T_c with a rate depending on the difference $T_m - T_c$. When the temperature is increased to T_{iq} , the kinetics become significantly slower. Actually, for a suitable choice of T_{iq} , the crystallization kinetics can be made as slow as wished and, for all practical purposes, virtually stopped. In summary, if the cooling and heating rates and the inverse quenching temperature are suitably chosen, a system constituted by a melt phase and a crystalline fraction produced at some lower temperature can be stabilized. This allows for the measurement of properties, such as the rheological ones, at constant degree of crystallization.

For the system under study, the inverse quenching temperature was selected on the basis of optical microscopy observations. It was determined as the temperature at which both nucleation and growth rates (and possibly the melting rate) were nearly reduced to zero.

The spherulitic growth rates of the PB177 were measured in the range from 91 to 108 °C by means of optical microscopy and successive image analysis. Samples were always annealed at 160 °C for 10 min and then cooled (−20 °C/min) to the crystallization temperature. The spherulitic radius vs time curves were found to be linear at all temperatures. Their slope, G , was therefore taken as the isothermal spherulitic growth rate. To measure the growth rate at the highest temperatures (namely 106, 107, 108 °C) with the best possible accuracy, a different procedure was adopted. In fact, as temperature approaches the thermodynamic melting point, induction times, i.e., the time necessary for nuclei formation, become exceedingly long. As a consequence, spherulites of observable size cannot be even detected within acceptable experimental times. For this reason, samples were first cooled to 96 °C and kept at this temperature for 30 min in order to produce spherulites of sufficiently large size. The system was then heated to the desired crystallization temperature, and the spherulitic growth was measured.

Radial growth rates as a function of the crystallization temperature are reported in Figure 6. Data obtained at high temperatures with the above-described two-step procedure seem to agree well with those determined at the lower temperature by means of the standard procedure. The results of Figure 6 are consistent with those already reported in the literature for

other PB grades.^{22,24} The high-temperature data indicate that the growth rate can be reduced to extremely low values. Above 110 °C, however, some onset of spherulite remelting was also observed. For these reasons an optimum inverse quenching temperature of 109 °C was chosen.

5.2. Degree of Crystallization. As it was already discussed in the previous section, a direct calorimetric measurement of α in the early stages of crystallization at temperatures investigated in this work was not possible, due to the extremely low heat fluxes. For this reason, crystallinity was measured on the basis of the time evolution of the elastic modulus by assuming a direct proportionality between α and G' as expressed by eq 1 already reported in the Introduction. This procedure has been widely used to characterize crystallization kinetics.^{1,4,25,26} A significant problem related to this choice is that the elastic modulus is frequency-dependent. It is well-known, however, that at low frequencies the storage modulus is more sensitive to any structural or thermal changes in the system. On the basis of both practical convenience and the above considerations, eq 1 was evaluated at the frequency $\omega_f = 0.06$ rad/s. Such a frequency is the fundamental frequency used in the *Multiwave* tests performed at crystallization time t_c , just before the application of the inverse quenching (see below).

On the basis of the above procedure, the degree of crystallinity of the PB177 sample was determined at the crystallizing temperature $T_c = 94$ °C and at different stages of the crystallization process. In particular, at the critical gel point, a degree of crystallinity $\alpha_c = 1.29\%$ was found, thus confirming that gelation takes place during the early stages of crystallization. This value is somewhat consistent with others already reported in the literature. Pogodina and Winter⁶ found very low crystallinities at the gel point for a series of different polypropylenes. In their case, a different technique for the evaluation of α_c was used, based on extrapolation of the Avrami time to the low degrees of undercooling used for the rheological experiments. Values of α_c ranging between about 0.2 and 4% were found, depending on crystallization temperature and polymer sample.

5.3. Low-Frequency Viscoelastic Behavior. As the inverse quenching allows keeping a “frozen” system for long times, dynamic frequency sweeps down to very low frequencies could be performed in order to explore the rheological behavior of the crystallizing system at fixed degree of crystallization. The structural evolution of the samples was monitored using the following experimental protocol. After an annealing period of 10 min at $T_{ann} = 160$ °C, a cooling (−10 °C/min) to the crystallization temperature $T_c = 94$ °C was applied. The sample was kept at this temperature for a period $t_c - t_0$, where t_0 is the time at which the crystallization temperature has been achieved. Different values of the crystallization time t_c were selected, corresponding to conditions before, at, and after the critical gel point, the latter being determined according to the procedure already presented in section 4. At $t = t_c$ a heating to the “inverse quenching” temperature, $T_{iq} = 109$ °C, was applied. Extreme caution was paid to avoid temperature overshoots (and subsequent partial melting). For this reason, a two-step heating process was performed to reach T_{iq} , namely, a first heating ramp at 5 °C/min up to 104 °C, followed by a second slower ramp at 1 °C/min up to 109 °C. The temperature was then kept constant to allow for rheological measurements at constant crystallinity.

During the whole experiment a *Multiwave* test was performed in order to check the validity of the inverse quenching technique. As outlined in the previous section, the test was also used to determine the G' evolution and, therefore, the degree of crystallinity. One example is reported in Figure 7, where the

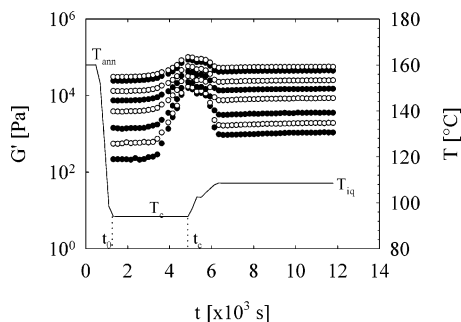


Figure 7. Storage modulus as a function of time during the inverse quenching experiment. The solid line represents the thermal history. Data have been collected by the *Multiwave* test. Data sets, from bottom to top, correspond to the following frequencies: 0.06, 0.12, 0.24, 0.6, 1.2, 2.4, 6.0, and 12.0 rad/s.

storage moduli at the frequencies imposed in the *Multiwave* test are plotted as a function of time along with the corresponding thermal history. After an induction time of about 2000 s at T_c , the modulus increase at all frequencies indicate the beginning of the crystallization process. When temperature is suddenly changed, the moduli stop growing and begin to decrease due to the corresponding increase in temperature. The achievement of the inverse quenching condition is proven by the long time constancy of the moduli at T_{iq} , indicating that no further crystallization (or remelting) is taking place over a time of at least 6000 s. Such a time was largely sufficient to perform dynamic frequency sweep (DFS) tests that covered a frequency window from 5×10^{-4} (using the *Multiwave* technique) to 10 rad/s. Following the indications given by Bove and Nobile,⁴ who measured the evolution of viscoelasticity of similar PB's during crystallization, a total strain less than or equal to 5% was always used in order to achieve a sufficiently high stress signal at all frequencies while remaining at all times within the linear viscoelastic regime.

The results of the frequency sweep tests obtained after inverse quenching are shown in Figure 8, where the storage modulus and the loss tangent are plotted as a function of frequency. Each data set corresponds to a given crystallization time and correspondingly (see section 5.2) to a given value of the degree of crystallization. Data corresponding to long crystallization times, i.e., complete crystallization, are also reported for comparison. In particular, data at $\alpha = 1.29$ correspond to the critical gel point, at least according to the procedure outlined in section 4, that is, when a constant $\tan \delta$ is observed at frequencies around 10^{-1} rad/s. It should be stressed that the results of Figure 8 have been obtained at the temperature of 109 °C but are the image of constant crystallinity states that were obtained at the temperature of 94 °C.

The storage modulus data in Figure 8a clearly indicate that an additional slower relaxation process appears in the very early stages of crystallization ($\alpha = 0.58\%$). Its existence has been speculated in the literature³ but, to our knowledge, is experimentally proven here for the first time. Data also indicate that the characteristic time for this process is around 1000 s and that a corresponding plateau for the storage modulus is clearly observable.

At the critical gel point ($\alpha = 1.29\%$) the slow relaxation process is almost hidden by the increasing elasticity of the material. The slight upturn in the G' curve at low frequencies demonstrates that the inverse quenching technique is not reliable when the system has reached the "gel condition", as already pointed out by Acierno and Grizzuti.¹⁴ This is not a dramatic

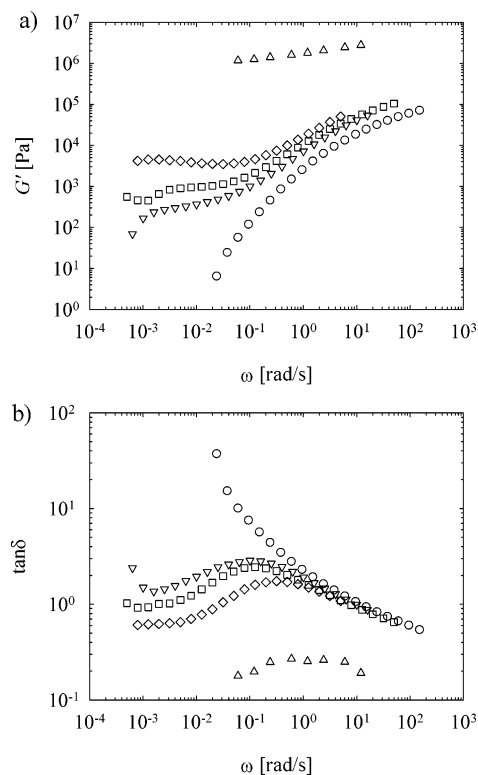


Figure 8. Linear viscoelasticity of PB177 at 109 °C after crystallization at 94 °C: (a) storage modulus; (b) loss tangent. Symbols denote different degrees of crystallization: (O) $\alpha = 0\%$ (melt); (V) $\alpha = 0.58\%$; (□) $\alpha = 1.29\%$; (◇) $\alpha = 2.8\%$; (△) $\alpha = 100\%$ (complete crystallization).

drawback, however, as after the gel time the crystallizing system approaches a nearly solidlike mechanical behavior.

Finally, the curve at $\alpha = 2.8\%$ clearly represents a system in which elasticity is near to predominate over the entire range of explored frequencies, as confirmed also by Figure 8b.

Notice that, when measurements are extended to such low frequencies, the concept itself of gel point must be revisited. In fact, typical gel point determinations for crystallizing polymers have been limited to higher frequencies, the gel point being typically detected in the frequency window 10^{-3} – 10^{-1} rad/s.^{3,6,7,9} Actually, the same criterion was also applied in this work to determine the characteristic crystallization times (see section 4, Figure 3 in particular).

At first sight, the viscoelastic behavior observed around the gel point could be explained in terms of the classical suspension theory. As crystallites grow in size, they will interact more and more, thus generating a gradual increase of all mechanical properties. Although a clear relation exists between crystallite growth and viscoelastic response, this simple picture is contradicted by the observation that the dramatic changes in viscoelasticity take place at extremely low values of the crystalline volume fraction. This point can be further confirmed by some considerations on the characteristic lengths involved in the process. Independent measurements¹⁷ provide the nucleation density, ν , of PB177 as $\nu \cong 4.7 \times 10^5$ nuclei/cm³ at the temperature of 94 °C. From this value, assuming a uniform distribution of nuclei, an estimate of the average distance between nuclei centers, ξ_0 , is obtained as

$$\xi_0 \cong \left(\frac{1}{\nu}\right)^{1/3} = 1.29 \times 10^{-2} \text{ cm} \quad (6)$$

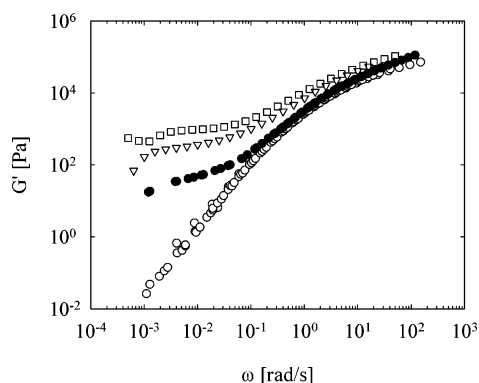


Figure 9. Storage modulus of PB177 at 109 °C after crystallization at 94 °C. Empty symbols as in Figure 8. Filled symbols refer to a completely molten sample filled with glass beads at an equivalent volume fraction $\alpha_{eq} = 24\%$.

Under the simplifying assumption that all nuclei form at the same time, the spherulite diameter during crystallization, D_{sph} can also be obtained from the relative crystallinity as

$$D_{sph} \cong \left(\frac{6V_{sph}}{\pi} \right)^{1/3} = \left(\frac{6\alpha X_{\infty}}{\pi\nu} \right)^{1/3} \quad (7)$$

where the volume of a single spherulite, V_{sph} , has been expressed in terms of the relative crystallinity, α , the maximum fraction of crystalline phase, X_{∞} , and the nuclei density. For PB, $X_{\infty} \cong 0.5$.²⁴ Therefore, at the critical gel point ($\alpha = 1.29\%$) one obtain $D_{sph} \cong 3.0 \times 10^{-3}$ cm. This would imply an average distance between spherulites, ξ , given by

$$\xi = \xi_0 - D_{sph} \cong 10^{-2} \text{ cm} \quad (8)$$

that is, $\xi \cong 100 \mu\text{m}$. Obviously, at such a large distance, very little interactions between crystallites is expected. The estimate given by eq 8 also rules out the possibility that the long relaxation dynamics observed in Figure 8 is due to chain bridging between adjacent spherulites. The average inter-spherulite distance is many orders of magnitude larger than the average coil size (the latter being in the order of a few tens of nanometers), which makes bridging an extremely unlikely event.

An even more convincing indication that the early stage microstructure cannot be merely reduced to a suspension of solid beads can be found in the data presented in Figure 9. Here, the crystallizing polymer is simulated by a suspension of glass beads immersed in the same PB177 molten sample. As already specified in the Experimental Section, beads have an average diameter of $60 \mu\text{m}$ and have been mixed to a volume fraction $X = 12\%$. Their number density is also comparable to the nuclei number density of the crystallizing sample. This would be equivalent to a crystalline polymer having an equivalent relative crystallinity $\alpha_{eq} = X/X_{\infty} \cong 24\%$. As for the pure melt, measurements were taken at the reference temperature of 140 °C and then reduced to 109 °C (the inverse quenching temperature where measurements of the crystallizing polymer were performed) by using the appropriate shift factor.

The results of Figure 9 clearly show that, although producing the same qualitative consequences, the presence of an order of magnitude larger amount of a noninteracting filler has much less effect in enhancing the low-frequency elasticity of the polymer.

6. Concluding Remarks

The experimental results presented in this paper give some relevant, although not conclusive, indications on the micro-

structure evolution during the early stages of crystallization. The poly(1-butene) here investigated clearly shows a liquid-to-solid transition under isothermal conditions, which is characterized by two main features. First, it takes place at surprisingly low degrees of crystallinity. Second, it is immediately preceded by the development of a long relaxation process, which has been experimentally detected here for the first time. Actually, the mere existence of a critical gel transition, as traditionally presented in earlier studies, could be questioned. A much more complex viscoelasticity evolution is revealed when sufficiently low frequencies are explored.

Although the buildup of a slow relaxation dynamics (and, therefore, of a correspondent microstructure) is strictly related to the ongoing crystallization process, our results show that it cannot be simply caused by the mere “space-filling” process due to the progressive increase of the crystalline phase. In fact, the rheologically observed transition takes place when the relative crystallinity is of the order of 1%. If spherulites just acted as solid particles suspended in the fluid, such a low volume fraction would hardly generate any change in the viscoelastic behavior of the crystallizing polymer. This point has been experimentally proven in this work by a direct comparison between the crystallizing polymer and a much more concentrated suspension of real hard spheres. The low crystallinity at the gel point simultaneously rules out the possibility that the elasticity of the diluted spherulite suspension is somewhat strengthened by polymer chain bridging between adjacent spherulites.

As both long-range (inter-spherulite) and short-range (chain bridging) interactions cannot be considered as the factors determining the polymer phase transition, we can only argue that some sort of coupling exists between the spherulites and the melt phase, which is able to generate the relevant viscoelastic changes during the initial crystallization steps. The nature of such a coupling, however, remains unclear, and certainly calls for more investigation. Leaving the floor to speculations, some observations could be attempted.

First, the rheological behavior of the crystallizing polymer, as shown in Figure 8, closely resembles that observed for polymers with long chain branching (LCB).²⁷ As the fraction of LCB is increased, a critical gel response is observed at intermediate frequencies. In fact, this apparent gel behavior is due to the partial overlapping between the (faster) relaxation of linear chains and the (slower) arm relaxation process. From this perspective one may speculate that, in the early stages of crystallization, polymer chains “grafted” at the spherulite surface may act as branching arms, thus analogously interacting with the linear, unconstrained chains that are still part of the amorphous phase. The concept that the polymer relaxation time is increased by the presence of nuclei acting as physical cross-links has been already used when modeling the rheology of flow-induced crystallization.^{28,29} Similar, interesting analogies can be also drawn with the viscoelastic behavior of multiarm star polymers³⁰ and of block copolymer micelles.³¹

From a completely different point of view, the strong change in the viscoelastic properties at very low crystallinity levels might be attributed to the presence of the so-called “dormant nuclei”. Such a term has been recently introduced by Janeschitz-Kriegl and co-workers³² to indicate stable nuclei that form in the melt at any given temperature below the melting point. It is argued, however, that the growth of such nuclei is prohibited by the strong increase of the surface tension at their ends due to the growing process itself. The growth of dormant nuclei, and therefore their actual detection, would become possible only after particular thermomechanical histories, such as the applica-

tion of strong flows. It goes without saying that the remarkable evolution of the viscoelastic properties during the early stages of crystallization, as measured in the present work, might constitute an indirect proof of the existence of the dormant nuclei.

As a final remark we want to stress that, whatever microstructural evolution is involved, the condition of a frequency-independent loss tangent at intermediate frequencies cannot be considered as the indication of a critical gel state in the crystallizing polymer, as it has been commonly reported in the literature. Rather, it should just be viewed as the indirect consequence of the growth of a slow relaxation mode and of its coupling with the melt viscoelastic response, similarly to what has been already observed for long-chain branched polymers.²⁷ For the latter case, a rigorous explanation of this coupling was recently provided.³³ For crystallizing systems, like those studied in the present work, the reasons for the observed behavior are not yet clear and remain the subject of further work.

Acknowledgment. We thank Prof. G. C. Alfonso of the University of Genoa, Italy, for providing the samples and making available the molecular weight and calorimetric data. The work is partially supported by the Italian Ministry of University under Project PRIN 2004–2005: “Control and Modeling of Morphology of Semicrystalline Polymers under Realistic Processing Conditions” and by the EU (network HUSC, RTN-2000-00017).

References and Notes

- (1) Khanna, Y. P. *Macromolecules* **1993**, *26*, 3639.
- (2) Teh, J. W.; Blom, H. P.; Rudin, A. *Polymer* **1994**, *35*, 1680.
- (3) Boutahar, K.; Carrot, C.; Guillet, J. *Macromolecules* **1998**, *31*, 1921.
- (4) Bove, L.; Nobile, M. R. *Macromol. Symp.* **2002**, *180*, 169.
- (5) Lin, Y. G.; Mallin, D. T.; Chien, J. C. W.; Winter, H. H. *Macromolecules* **1991**, *24*, 850.
- (6) Pogodina, N. V.; Winter, H. H. *Macromolecules* **1998**, *31*, 8164.
- (7) Acerno, S.; Grizzuti, N.; Winter, H. H. *Macromolecules* **2002**, *35*, 5043.
- (8) Richtering, H. W.; Gagnon, K. D.; Lenz, R. W.; Fuller, R. C.; Winter, H. H. *Macromolecules* **1992**, *25*, 2429.
- (9) Cossar, S.; Nichetti, D.; Grizzuti, N. *J. Rheol.* **2004**, *48*, 691.
- (10) Tanner, R. I. *J. Non-Newton. Fluid Mech.* **2002**, *102*, 397.
- (11) Tanner, R. I. *J. Non-Newton. Fluid Mech.* **2003**, *112*, 251.
- (12) Tanner, R. I.; Qi, F. *J. Non-Newton. Fluid Mech.* **2005**, *127*, 131.
- (13) Pogodina, N. V.; Lavrenko, V. P.; Srinivas, S.; Winter, H. H. *Polymer* **2001**, *42*, 9031.
- (14) Acerno, S.; Grizzuti, N. *J. Rheol.* **2003**, *47*, 563.
- (15) Horst, R. H.; Winter, H. H. *Macromolecules* **2000**, *33*, 7538.
- (16) TA Instruments, Rheology Application Notes, paper RN-8.
- (17) Data kindly provided by Professor G. C. Alfonso, University of Genoa, Italy.
- (18) Winter, H. H.; Mours, M. *Adv. Polym. Sci.* **1997**, *134*, 165.
- (19) Doi, M.; Edwards, S. F. *The Theory of Polymer Dynamics*; Clarendon Press: New York, 1986.
- (20) Cortazar, M.; Guzman, G. M. *Makromol. Chem., Macromol. Chem. Phys.* **1982**, *183*, 721–729.
- (21) Lauritzen, J. I.; Hoffman, J. D. *J. Res. Natl. Bur. Stand. A* **1960**, *64*, 73.
- (22) Kishore, K.; Vasanthakumari, R. *Colloid Polym. Sci.* **1988**, *266*, 999.
- (23) Nichetti, D.; Cossar, S.; Grizzuti, N. *J. Rheol.* **2005**, *49*, 1361.
- (24) Braun, J.; Pillichshammer, D.; Eder, G.; Janeschitz-Kriegl, H. *Polym. Eng. Sci.* **2003**, *43*, 180.
- (25) Carrot, C.; Guillet, J.; Boutahar, K. *Rheol. Acta* **1993**, *32*, 566.
- (26) Vleeshouwers, S.; Meijer, H. E. H. *Rheol. Acta* **1996**, *35*, 391.
- (27) Robertson, C. G.; García-Franco, C. A.; Srinivas, S. *J. Polym. Sci., Polym. Phys.* **2003**, *42*, 1671.
- (28) Zuidema, H.; Peters, G. W. M.; Meijer, H. E. H. *Macromol. Theory Simul.* **2001**, *10*, 447.
- (29) Peters, G. W. M.; Swartjes, F. H. M.; Meijer, H. E. H. *Macromol. Symp.* **2002**, *185*, 277.
- (30) Vlassopoulos, D.; Fytas, G.; Pakula, T.; Roovers, J. *J. Phys.: Condens. Matter* **2001**, *13*, R855.
- (31) Watanabe, H. *Acta Polym.* **1997**, *48*, 215.
- (32) Janeschitz-Kriegl, H.; Ratajski, E. *Polymer* **2005**, *46*, 3856.
- (33) Kapnistos, M.; Vlassopoulos, D.; Roovers, J.; Leal, L. G. *Macromolecules* **2005**, *38*, 7852.

MA0518510